2021

Praseodymium Mid-Infrared Emission In AlF3-Based Glass Sensitized By Ytterbium

Jiquan Zhang
Harbin Engineering University, China

Mo Liu
Harbin Engineering University, China

Jin Yu
Harbin Engineering University, China

See next page for additional authors

Recommended Citation

Zhang, J., Mo Liu. & Yu, J. (2021). Praseodymium Mid-Infrared Emission In AlF3-Based Glass Sensitized By Ytterbium. *Optics Express*, vol. 29, no. 21, pg. 34166-34174. doi:10.1364/OE.438935

Research Article | Vol. 29, No. 21 / 11 Oct 2021 / Optics Express 34166
Optics EXPRESS

Praseodymium mid-infrared emission in AlF_3-based glass sensitized by ytterbium

JIQUAN ZHANG,[1] MO LIU,[1] JIN YU,[1] RUICONG WANG,[1] SHIJIE JIA,[1] ZIJUN LIU,[2] GERALD FARRELL,[3] SHUNBIN WANG,[1,5] AND PENGFEI WANG[1,4,6]

[1]*Key Lab of In-Fiber Integrated Optics of Ministry of Education of China, Harbin Engineering University, Harbin 150001, China*
[2]*Laboratory of Infrared Materials and Devices, Advanced Technology Research Institute, Ningbo University, Ningbo 315211, China*
[3]*Photonics Research Center, Technological University Dublin, Grangegorman Campus, Dublin 7, Ireland*
[4]*Key Laboratory of Optoelectronic Devices and Systems of Ministry of Education and Guangdong Province, College of Optoelectronic Engineering, Shenzhen University, Shenzhen 518060, China*
[5]*shunbinwang@hrbeu.edu.cn*
[6]*pengfei.wang@tudublin.ie*

Abstract: Broadband emission was obtained over 2.6 to 4.1 μm (Pr^{3+}: $^1G_4 \rightarrow {}^3F_4$, $^3F_3$) in AlF_3-based glass samples doped with different concentrations of praseodymium and 1 mol% ytterbium using a 976 nm laser pump. An efficient energy transfer process from Yb^{3+}: $^2F_{5/2}$ to Pr^{3+}: $^1G_4$ was analyzed through emission spectra and fluorescence lifetime values. The absorption and emission cross-sections were calculated by Füchtbauer-Ladenburg and McCumber theories and a positive gain can be obtained when P>0.3. To the best of the authors' knowledge, this work represents the first report of broadband mid-infrared emission of Pr^{3+} in an AlF_3-based glass. The results show that praseodymium doped AlF_3-based glass sensitized by ytterbium could be a promising candidate for fiber lasers operating in mid-infrared region.

1. Introduction

Mid-infrared (MIR) lasers in the range of 2-5 μm have attracted significant scientific interest as their wavelength range coincides with minimum attenuation in the atmospheric transmission window. In addition, the presence of many absorption peaks for gas and organic molecules in the same wavelength region guarantees the application of MIR lasers in many fields, including aerospace communication [1], atmospheric monitoring [2], spectroscopy [3] and national defense [4]. There are two distinct technological approaches to the implementation of MIR lasers. The first one is based on nonlinear optical effects, including optical parametric oscillation (OPO) [5] and difference frequency generation (DFG) [6]. However, this form of laser usually suffers from significant complexity, low electro-optical efficiency, and a complicated OPO crystal preparation process. Alternatively, MIR lasers can also be realized directly through gain materials including quantum well (QW) semiconductors [7] and transition metal (TM) doped II-IV semiconductors [8]. QW lasers are high-beam-quality devices, while TM-doped II-IV semiconductor lasers suffer from dramatically reduced laser output efficiency at higher temperatures [9]. Solid state lasers based on these materials have been extensively studied and have already been commercialized.

However, compared with the above techniques, rare earth (RE) doped MIR fiber lasers exhibit significant advantages including a greater spectral range, better pump efficiency, higher transmittance, stability, improved portability and easier-integration, etc. [10]. Fluoride and chalcogenide glasses are known as suitable materials for MIR fiber lasers. Of particular note very recently, there has been some progress in lasing beyond 5 μm, that has been achieved in chalcogenide glass fibers thanks to its lower phonon energy, greatly expanding the potential

#438935 https://doi.org/10.1364/OE.438935
Journal © 2021 Received 27 Jul 2021; revised 11 Sep 2021; accepted 18 Sep 2021; published 5 Oct 2021

Optics EXPRESS

applications of RE doped fiber lasers [11,12]. At present, most 2-5 μm MIR fiber lasers use fluoride glass fibers doped with Er^{3+}, Dy^{3+} and Ho^{3+} to produce an output in the range of 2.7-3.9 μm in fluorozirconate and fluoroindate materials, which are easy to fabricate and possess wide transmission windows and higher rare earth solubility than chalcogenide glasses, moreover, they also show high transmittances in this region compared to chalcogenide [13]. ZBLAN (ZrF_4-BaF_2-LaF_3-AlF_3-NaF) glass is one of the most widely studied host materials since 1985 [14,15]. Some significant research advances have been made in RE-doped ZBLAN materials in the past few years [13]. In recent years, fluoroindate material with its lower phonon energy has attracted attention for example the demonstration of a 197 mW fiber laser at the wavelength of 3.9 μm [16]. However, generally speaking, fluorozirconate and fluoroindate fibers suffer from severe deliquescence, which limits their applications in many fields.

AlF_3-based glasses possess much higher chemical and thermal stability, exhibit superior moisture resistance performance compared to ZBLAN glass [17,18], and have been employed in VIS-NIR-MIR lasers. In 2010, a visible yellow laser output was realized in Dy^{3+}-doped AlF_3-based glass fibers [19]. In 2000, Nd^{3+}-doped AlF_3-based glass fibers were utilized for a 1.3 μm fiber amplifier [20]. Very recently, some authors of our group successfully demonstrated a ~2.86 μm MIR laser in Ho^{3+}/Pr^{3+} co-doped AlF_3-based glass fibers with output powers up to 1 W [21,22], indicating that AlF_3-based glass has great potential in the field of mid-infrared lasers.

RE-doped fluoride fiber lasers operating at ~3.5 μm usually require a complex setup, and are limited by the pump efficiency and pump source availability [23,24]. Therefore, it is necessary to develop novel rare-earth doped materials that could be excited by commonly available commercial laser devices operating at ~808 nm or ~980 nm to produce an intense ~3.5 μm MIR emission.

In this study, intense 2.6-4.1 μm broadband emission peaked at 3.46 nm is realized in Pr^{3+}/Yb^{3+} co-doped AlF_3-based glass pumped by a 976 nm laser diode, demonstrating that there is an efficient energy transfer process from Yb^{3+} to Pr^{3+}. The calculated results using Judd-Ofelt and Füchtbauer-Ladenburg theories give a more detailed analysis for this material.

2. Experiments

The AlF_3-based glass compositions used in the experiment can be expressed in terms of molecular ratio as 30AlF_3-10BaF_2-19CaF_2-(9.5-x-y)YF_3-12.5SrF_2-3.5MgF_2-3LiF-10ZrF_4-2.5PbF_2-xPrF_3-yYbF_3 (x=0, 0.1, 0.2, 0.3, 0.5, 1, 2, 3; y=0, 1). Using high-purity and dehydrated fluorides, the AlF_3-based glasses were fabricated using a conventional melt-quenching technique. The mixture was heated and melted in a platinum crucible at 900 °C for 60 minutes in a glove box with ultra-dry N_2 to reduce the content of hydroxyl impurities. The melt was then cast onto a brass plate preheated at 370 ℃ and then annealed for 3 hours. Glass samples were then cut and polished with dimensions 10×10×2 mm for subsequent measurements.

Absorption and transmission spectra in the range of 200−2500 nm and 2500−9000 nm were recorded using a Perkin Elmer Lambda 750 UV–VIS–NIR spectrophotometer and Perkin Elmer Fourier-transform infrared (FTIR) spectrometer, respectively. Fluorescence spectra were measured using computer controlled Zolix Omni-λ300i monochromators and spectrographs which were equipped with InGaAs and InSb detectors to suit the wavelength range in use. The pump source was a commercial 976 nm multimode fiber laser (BWT, K976A02RN). The luminescence decay curves were measured using an optical parametric oscillator (Horizon II OPO) with a pulse width of 6 μs and repetition rate of 10 Hz. A spectrometer (Synerjy 1000M) and a digital phosphor oscilloscope (DP04104B) were used to detect and record the fluorescence decay curves. All measurements were conducted at room temperature.

3. Results and discussions

AlF_3-based glass samples doped with 1 mol% Yb^{3+} and with different concentrations of Pr^{3+} were synthesized. The absorption and transmission spectra of these glasses are shown in Fig. 1.

Optics EXPRESS

The absorption peaks in Fig. 1(a) correspond to the transitions from ground level to excited energy levels of Yb^{3+} and Pr^{3+}, and the overlapping peak near 980 nm indicates that a ~980 nm LD could be used as the pump.

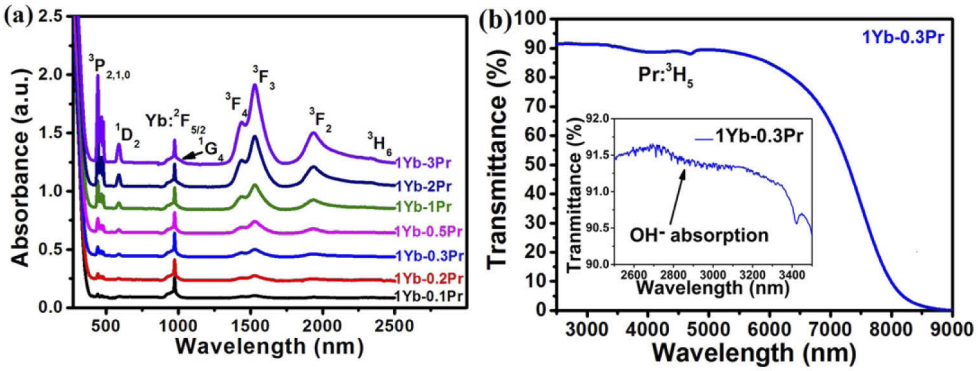

Fig. 1. (a) The absorption spectra, and (b) transmission spectrum of Pr^{3+}/Yb^{3+} co-doped AlF_3-based glasses. Inset: an enlargement spectrum from 2500 nm to 3500 nm.

As shown in Fig. 1(b), the average transmittance is ~92% for wavelengths shorter than 5 μm, and the cutoff wavelength is 9 μm, proving that the AlF_3-based glass can be utilized for mid-infrared applications. The inset shows the spectral region near 3μm, and the very weak absorption peak of OH^- is evidence that the OH^- content of the AlF_3-based glass was very low. The absorption coefficient of OH^- calculated by $\alpha_{OH-}=\ln(T_0/T)/l$ is 0.0078 cm^{-1}, lower than that of fluorozirconate (0.031cm^{-1}) [25] and fluoroindate (0.06 cm^{-1}) [26], where T_0 is the maximum transmittance, T the transmittance at λ~3 μm and l the thickness of the glass sample.

The energy level diagram of Pr^{3+} and Yb^{3+} is shown in Fig. 2.

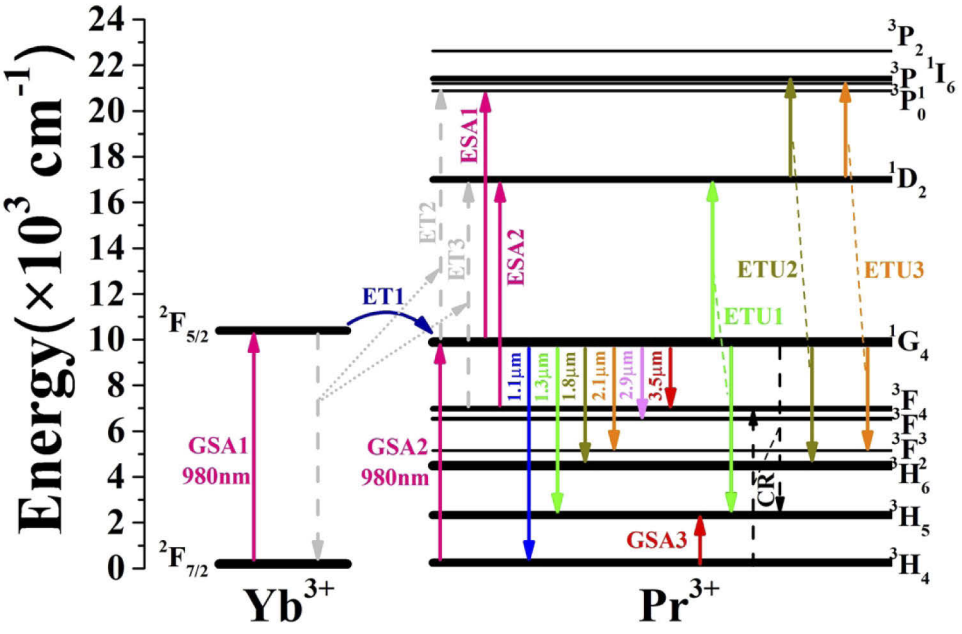

Fig. 2. The energy level diagram of Pr^{3+}, Yb^{3+} ions and the infrared emission mechanisms.

Optics EXPRESS

Although Pr^{3+} ions can be pumped to the $^1G_4$ level by ground state absorption (GSA2), the efficiency is very low [27], while Yb^{3+} ions can efficiently absorb ~980 nm photon energy through the GSA1 process. By introducing Yb^{3+}, the photon energy can be transferred to Pr^{3+} ions through the energy transfer (ET1) process. After being pumped to $^1G_4$, several down-conversion emissions from the $^1G_4$ level to lower levels occurred, emitting photons at 1.1, 1.3, 1.8, 2.1, 2.9 and 3.5 μm. Meanwhile, the excited Pr^{3+} ions can absorb ~980 nm photon energy and transit to $^3P_0$ and $^1D_2$ levels by excited state absorption (ESA1, ESA2) and energy transfer processes (ET2, ET3) [28]. Then the populations on higher levels will relax to the $^1G_4$ level, resulting in more efficient emissions.

To evaluate the ET1 efficiency from Yb^{3+} to Pr^{3+}, the luminescence decay curves of Yb^{3+}:$^2F_{5/2}$ were recorded with pumping by a 976 nm LD, as shown in Fig. 3(a). One of the typical curves of 1Yb-0.3Pr is shown in the inset.

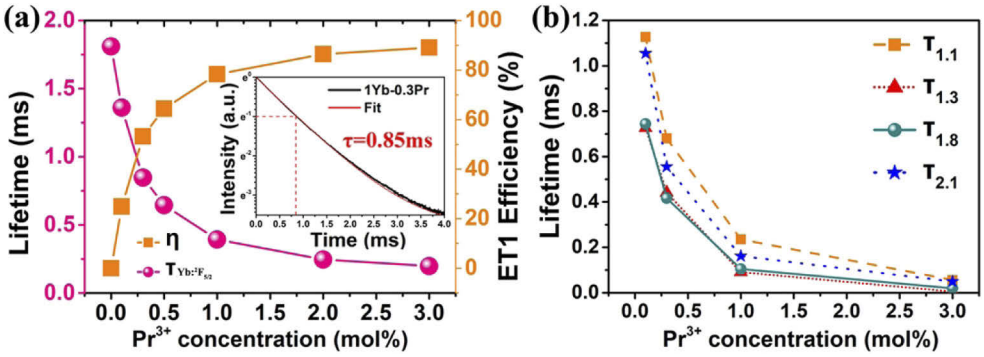

Fig. 3. (a) The dependence of Yb^{3+}:$^2F_{5/2}$ lifetime and energy transfer efficiency on Pr^{3+} concentration. Inset: The luminescence decay curve of Yb^{3+}:$^2F_{5/2}$ in 1Yb-0.3Pr sample. (b) The lifetime of Pr^{3+}: $^1G_4 \rightarrow {}^3H_4$, $^3H_5$, $^3H_6$ and $^3F_2$.

The energy transfer efficiency can be calculated using the following equation:

$$\eta = 1 - \frac{\tau_{1\mathrm{Yb\text{ - }xPr}}}{\tau_{1\mathrm{Yb}}} \tag{1}$$

where $\tau_{1\mathrm{Yb-xPr}}$ is the luminescence lifetime of Yb^{3+}:$^2F_{5/2}$ and the Pr^{3+} concentration is x. It can be seen that the lifetime of the $^2F_{5/2}$ level decreases as the Pr^{3+} concentration increases, and that the ET1 efficiency increases to its maximum value of 89% at 3 mol%, proving the efficiency of the ET1 process. Figure 3(b) shows the lifetimes of the transitions from $^1G_4$ to $^3H_4$, $^3H_5$, $^3H_6$ and $^3F_2$ levels in Pr^{3+} ions. The decreases can be attributed to the energy transfer up-conversion (ETU1, ETU2, and ETU3) and cross-relaxation (CR) processes between the Pr^{3+} ions [29], which would increase accordingly as a result of the higher doping concentration and the shorter distance between ions. As shown in Fig. 2, these processes together lead to a reduction of the populations on the $^1G_4$ level. Furthermore, the Pr^{3+} wide ground state absorption from $^3H_4 \rightarrow {}^3H_5$ (GSA3) in the range of 2.5-5.7 μm can also cause a depopulation effect on the $^1G_4$ level [30].

Compared with Yb^{3+}, Pr^{3+} has weak absorption peaks at 976 nm, as shown in Fig. 4(a). It is crucial to introduce Yb^{3+} as a sensitizer to enhance the pump efficiency due to its strong absorption in this wavelength region. Using a 976 nm LD as the pump source, the MIR emission spectra of Pr^{3+} single-doped and Pr^{3+}/Yb^{3+} co-doped AlF_3-based glasses were recorded and are shown in Fig. 4(b). The 2.9 and 3.5 μm MIR emission peaks can be attributed to the transitions of $^1G_4 \rightarrow {}^3F_3$ and $^1G_4 \rightarrow {}^3F_4$, respectively. Figure 4(b) shows that the 2.6-4.1 μm MIR emission intensity is greatly improved by a factor of 16 due to the ET1 process from the Yb^{3+} ions to

Optics EXPRESS

Pr^{3+} ions, clearly proving that 976 nm is a suitable pumping wavelength in Pr^{3+}/Yb^{3+} co-doped glasses. These energy transfer processes greatly enhance the populations on the Pr^{3+}: $^1G_4$ level and are therefore of great benefit in the generation of intense MIR emissions.

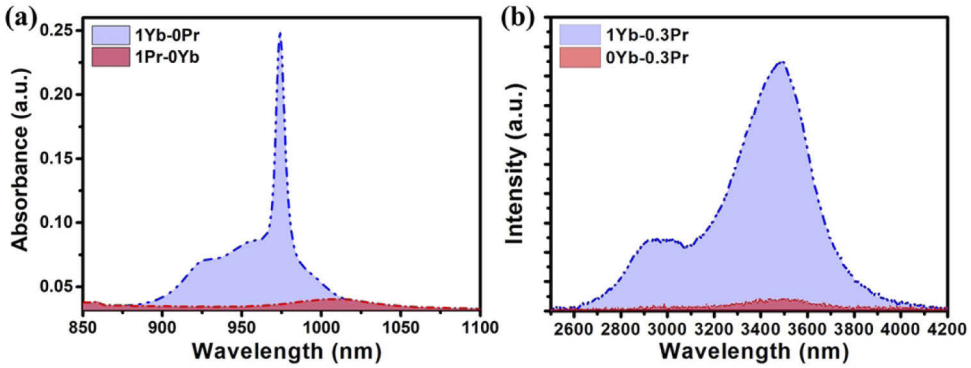

Fig. 4. (a) Absorption spectra near 980 nm in Yb^{3+} and Pr^{3+} single-doped AlF_3-based glasses. (b) The ~3.5 μm (from 2.6 to 4.1 μm) mid-infrared emission spectra of Pr^{3+}/Yb^{3+} co-doped and Pr^{3+} single-doped AlF_3-based glasses.

Figure 5 shows the emissions in the MIR ($^1G_4 \rightarrow {}^3F_3$, $^3F_4$) and near-infrared (NIR) range ($^1G_4 \rightarrow {}^3H_4$, $^3H_5$, $^3H_6$, $^3F_2$). It is worth noting that the characteristics of the radiative transitions mentioned above show evidence of concentration quenching. For NIR emissions at 1.1 and 2.1 μm, the concentration needed for maximum intensity is 0.1 mol%, while that for the emission at 1.32 μm is 0.5 mol%. As for the emission near 1.8 μm, it has almost equal intensities when the Pr^{3+} concentrations are 0.2 to 0.5 mol%. For the MIR emissions, the concentration needed for the maximum intensity is 0.3 mol%. Though 3.5 μm emission ($^1G_4 \rightarrow {}^3F_4$) is easily affected by GSA3 process, an efficient emission could be achieved with an appropriate doping concentration [31]. Compared with ZBLAN glass (2.8-3.95 μm [30]; 3-3.9 μm [31]), the transitions from $^1G_4 \rightarrow {}^3F_3$ and $^3F_4$ in AlF_3-based glass have a wider width.

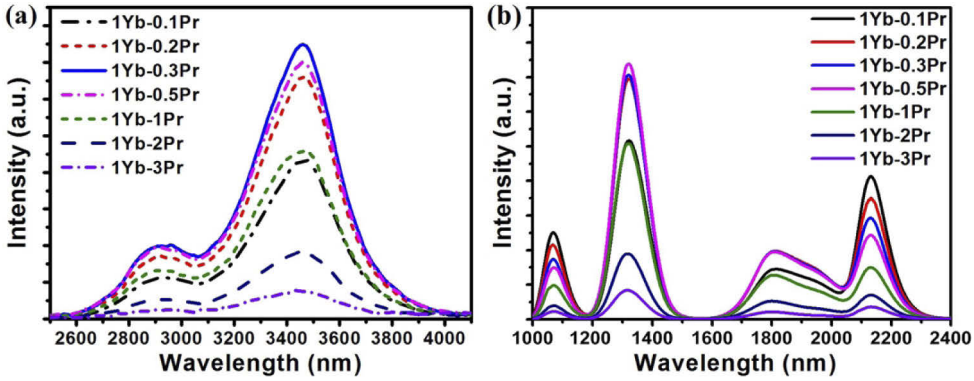

Fig. 5. The (a) Mid-infrared, and (b) near-infrared emission spectra of Pr^{3+}/Yb^{3+} co-doped AlF_3-based glasses with different concentration of Pr^{3+}.

Figure 6 shows normalized mid-infrared emission spectra of AlF_3-based glasses with different RE dopants. Several RE ions can generate radiative emissions corresponding to the transitions of Er^{3+}:$^4I_{11/2} \rightarrow {}^4I_{13/2}$, Dy^{3+}:$^6H_{13/2} \rightarrow {}^6H_{15/2}$, Ho^{3+}:$^5I_6 \rightarrow {}^5I_7$, Pr^{3+}:$^1G_4 \rightarrow {}^3F_4$, Er^{3+}:$^4F_{9/2} \rightarrow {}^4I_{9/2}$, Ho^{3+}:$^5I_5 \rightarrow {}^5I_6$. These transitions have small energy gaps, thus when the phonon energy of the

Optics EXPRESS

host material is relatively large, it will result in a high non-radiative decay rate, according to the modified non-radiative decay theory proposed by V. Dijk and M. Schuurmans [32]. Consequently, it is useful to note that it is possible to suppress the non-radiative relaxation process by reducing the phonon energy of the host material.

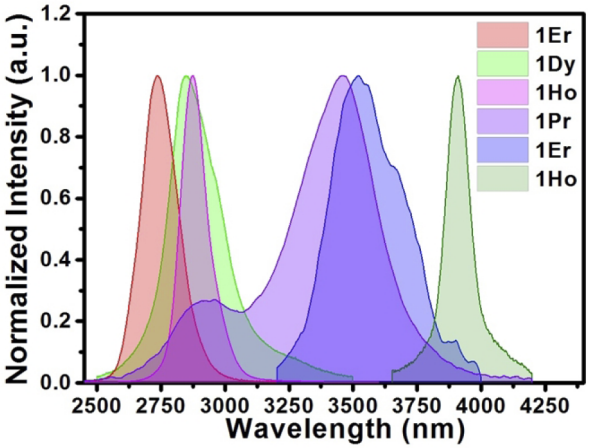

Fig. 6. The normalized mid-infrared emission spectra of AlF_3-based glasses with different rare earth dopants in the region of 2500-4200 nm.

The emission results indicate that AlF_3-based glass with low phonon energy (615 cm^{-1}) is a suitable host for doping in order to emit photons in the MIR region. It is also worth noting that the emission band of Pr^{3+} can cover the range of 2.6 to 4.1 μm, which is much wider than that of other RE ions. This broad bandwidth could be a valuable asset in the implementation of wavelength-tunable MIR lasers.

Judd-Ofelt (J-O) theory is usually applied to evaluate the emission properties of RE dopants and the nature of host matrixes [33]. The J-O parameters of Pr^{3+} ions $\Omega_{2,4,6}$ were calculated to be 0.20×10^{-20}, 3.96×10^{-20} and 5.32×10^{-20} cm^2, respectively. Other radiative properties including radiative transition probabilities, energy level lifetimes and fluorescence branch ratios were also calculated. The results of transitions from $^1G_4$ to lower levels are shown in Table 1.

Table 1. Radiative properties of transitions from $^1G_4$ to lower levels.

Transitions	Arad (s^{-1})	Lifetimes (ms)	Branch Ratio (%)
$^1G_4 \rightarrow {}^3F_4$	15.03	2.3	3
$^3F_3$	2.73		1
$^3F_2$	2.58		1
$^3H_6$	93.29		21
$^3H_5$	283.28		65
$^3H_4$	38.80		9
$\Omega_2=0.2\times10^{-20}$ cm^2	$\Omega_4=3.96\times10^{-20}$ cm^2		$\Omega_6=5.32\times10^{-20}$ cm^2

Based on the above experimental data and calculation results, the emission and absorption cross-sections were calculated using Füchtbauer-Ladenburg and McCumber theories [34,35], as shown in Fig. 7. The calculated peak values of the emission and absorption cross-sections are 3.21×10^{-21} cm^2 and 3.89×10^{-21} cm^2, respectively, showing the emission cross-section of Pr^{3+} near 3.5 μm in AlF_3-based glass material is much higher than that of ZBLAN material doped

Optics EXPRESS

with Er^{3+} or Ho^{3+}. This confirms the potential of Pr^{3+} in AlF_3-based glass materials as a new approach to implementing MIR lasers [36,37].

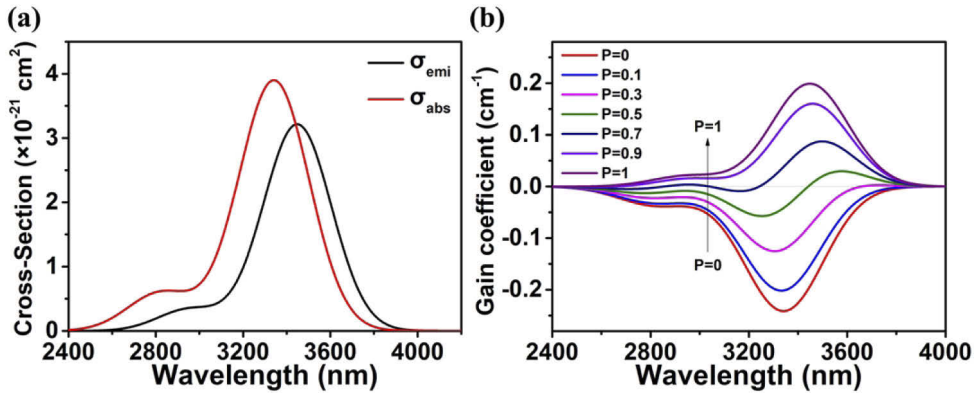

Fig. 7. (a) The absorption and emission cross-sections of Pr^{3+}:$^1G_4 \rightarrow {}^3F_3$, $^3F_4$ in AlF_3-based glass. (b) The gain spectra of Pr^{3+}:$^1G_4 \rightarrow {}^3F_3$, $^3F_4$ in AlF_3-based glass.

The gain properties of laser medium can be estimated from its gain coefficient, which can be derived from the emission and absorption cross-sections. The gain coefficient of Pr^{3+}/Yb^{3+} co-doped AlF_3-based glass was calculated and the resulting values versus wavelength are shown in Fig. 7(b). A positive gain coefficient can be obtained when P≥0.3 (P = the population of the upper energy levels/the population of total energy levels) beyond 3659.4 nm, indicating that it requires a relatively low pump power threshold to generate laser output in a Pr^{3+}/Yb^{3+} co-doped AlF_3-based glasses fiber.

4. Conclusion

In summary, 2.6-4.1 μm MIR emissions were successfully achieved in Pr^{3+}/Yb^{3+} co-doped AlF_3-based glasses under excitation by a 976 nm LD. The optimal Pr^{3+} concentration was experimentally determined to be 0.3 mol% for MIR emission. Based on the measured luminescence decay curves and lifetimes, the transition mechanism and energy transfer efficiency were ascertained. After calculating the emission and absorption cross-sections, the gain coefficient was also calculated. The results demonstrate that Pr^{3+}/Yb^{3+} co-doped AlF_3-based glass shows good potential for use in 2.6-4.1 μm MIR fiber lasers.

Funding. National Natural Science Foundation of China (61935006, 62005060, 61905048, 62090062, 61805074); National Key Research and Development Program of China (2020YFA0607602); Shenzhen Technical Project (JCYJ20190808173619062); 111 project to the Harbin Engineering University (B13015); Heilongjiang Touyan Innovation Team Program.

Disclosures. The authors declare no conflicts of interest.

Data availability. Data underlying the results presented in this paper are not publicly available at this time but may be obtained from the authors upon reasonable request.

References

1. Y. Ohyama, T. Onaka, H. Matsuhara, T. Wada, W. Kim, N. Fujishiro, K. Uemizu, I. Sakon, M. Cohen, M. Ishigaki, D. Ishihara, Y. Ita, H. Kataza, T. Matsumoto, H. Murakami, S. Oyabu, T. TanabÉ, T. Takagi, M. Ueno, F. Usui, H. Watarai, C. P. Pearson, N. Takeyama, T. Yamamuro, and Y. Ikeda, "Near-Infrared and Mid-Infrared Spectroscopy with the Infrared Camera (IRC) for AKARI," Publications of the Astronomical Society of Japan **59**, S411–S422 (2007).
2. C. Clerbaux, A. Boynard, L. Clarisse, M. George, J. Hadji-Lazaro, H. Herbin, D. Hurtmans, M. Pommier, A. Razavi, S. Turquety, C. Wespes, and P. F. Coheur, "Monitoring of atmospheric composition using the thermal infrared IASI/MetOp sounder," Atmos. Chem. Phys. **9**(16), 6041–6054 (2009).
3. F. Keilmann, C. Gohle, and R. Holzwarth, "Time-domain mid-infrared frequency-comb spectrometer," Opt. Lett. **29**(13), 1542–1544 (2004).

Optics EXPRESS

4. F. Hanson, P. Poirier, and M. A. Arbore, "Single-frequency mid-infrared optical parametric oscillator source for coherent laser radar," Opt. Lett. **26**(22), 1794–1796 (2001).
5. P. A. Budni, L. A. Pomeranz, M. L. Lemons, C. A. Miller, J. R. Mosto, and E. P. Chicklis, "Efficient mid-infrared laser using 1.9-μm-pumped Ho:YAG and ZnGeP2 optical parametric oscillators," J. Opt. Soc. Am. B **17**(5), 723–728 (2000).
6. W. Chen, J. Cousin, E. Poullet, J. Burie, D. Boucher, X. Gao, M. W. Sigrist, and F. K. Tittel, "Continuous-wave mid-infrared laser sources based on difference frequency generation," C. R. Phys. **8**(10), 1129–1150 (2007).
7. J. I. Malin, J. R. Meyer, C. L. Felix, J. R. Lindle, L. Goldberg, C. A. Hoffman, F. J. Bartoli, C. H. Lin, P. C. Chang, S. J. Murry, R. Q. Yang, and S. S. Pei, "Type II mid-infrared quantum well lasers," Appl. Phys. Lett. **68**(21), 2976–2978 (1996).
8. S. Mirov, V. Fedorov, I. Moskalev, M. Mirov, and D. Martyshkin, "Frontiers of mid-infrared lasers based on transition metal doped II–VI semiconductors," J. Lumin. **133**, 268–275 (2013).
9. I. T. Sorokina, "Cr^{2+}-doped II–VI materials for lasers and nonlinear optics," Opt. Mater. **26**(4), 395–412 (2004).
10. S. D. Jackson, "Towards high-power mid-infrared emission from a fibre laser," Nat. Photonics **6**(7), 423–431 (2012).
11. J. Nunes, R. Crane, D. Furniss, Z. Tang, D. Mabwa, B. Xiao, T. Benson, M. Farries, N. Kalfagiannis, and E. Barney, "Room temperature mid-infrared fiber lasing beyond 5 μm in chalcogenide glass small-core step index fiber," Opt. Lett. **46**(15), 3504–3507 (2021).
12. V. Shiryaev, M. Sukhanov, A. Velmuzhov, E. Karaksina, T. Kotereva, G. Snopatin, B. Denker, B. Galagan, S. Sverchkov, and V. Koltashev, "Core-clad terbium doped chalcogenide glass fiber with laser action at 5.38 μm," J. Non-Cryst. Solids **567**, 120939 (2021).
13. W. C. Wang, B. Zhou, S. H. Xu, Z. M. Yang, and Q. Y. Zhang, "Recent advances in soft optical glass fiber and fiber lasers," Prog. Mater. Sci. **101**, 90–171 (2019).
14. L. E. Busse, G. Lu, D. C. Tran, and G. H. Sigel Jr, "A Combined DSC/Optical Microscopy Study of Crystallization in Fluorozirconate Glasses upon Cooling from the Melt," Mater. Sci. Forum **5-6**, 219–228 (1985).
15. X. Zhu and N. Peyghambarian, "High-Power ZBLAN Glass Fiber Lasers: Review and Prospect," Adv. OptoElectron. **2010**, 501956 (2010).
16. F. Maes, V. Fortin, S. Poulain, M. Poulain, J.-Y. Carrée, M. Bernier, and R. Vallée, "Room-temperature fiber laser at 3.92 μm," Optica **5**(7), 761–764 (2018).
17. D. Ehrt, "Fluoroaluminate glasses for lasers and amplifiers," Current Opinion in Solid State and Materials Science **7**(2), 135–141 (2003).
18. Y. Dai, K. Takahashi, and I. Yamaguchi, "Water Corrosion Behavior of Fluoroaluminate Glass," J. Am. Ceram. Soc. **78**, 183 (2010).
19. Y. Fujimoto, O. Ishii, and M. Yamazaki, "Yellow laser oscillation in Dy^{3+}-doped waterproof fluoro-aluminate glass fibre pumped by 398.8 nm GaN laser diodes," Electron. Lett. **46**(8), 586–587 (2010).
20. M. Naftaly and A. Jha, "Nd^{3+}-doped fluoroaluminate glasses for a 1.3 μm amplifier," J. Appl. Phys. **87**(5), 2098–2104 (2000).
21. S. Wang, J. Zhang, N. Xu, S. Jia, G. Brambilla, and P. Wang, "2.9 μm lasing from a Ho^{3+}/Pr^{3+} co-doped AlF3-based glass fiber pumped by a 1150 nm laser," Opt. Lett. **45**(5), 1216–1219 (2020).
22. M. Liu, J. Zhang, N. Xu, X. Tian, S. Jia, S. Wang, G. Brambilla, and P. Wang, "Room-temperature watt-level and tunable ~3 μm lasers in Ho^{3+}/Pr^{3+} co-doped AlF_3-based glass fiber," Opt. Lett. **46**(10), 2417–2420 (2021).
23. H. Többen, "Room temperature cw fibre laser at 3.5 μm in Er^{3+}-doped ZBLAN glass," in *Electronics Letters* (Institution of Engineering and Technology, 1992), pp. 1361–1362.
24. O. Henderson-Sapir, J. Munch, and D. J. Ottaway, "New energy-transfer upconversion process in Er^{3+}: ZBLAN mid-infrared fiber lasers," Opt. Express **24**(7), 6869–6883 (2016).
25. F. Huang, T. Ying, H. Li, S. Xu, and J. Zhang, "Ho^{3+}/Er^{3+} co-doped fluoride glass sensitized by Tm^{3+} pumped by a 1550 nm laser diode for efficient 2.0 μm laser applications," Opt. Lett. **40**(18), 4297–4300 (2015).
26. L. Gomes, V. Fortin, M. Bernier, R. Vallée, S. Poulain, M. Poulain, and S. D. Jackson, "The basic spectroscopic parameters of Ho3+-doped fluoroindate glass for emission at 3.9 μm," Opt. Mater. **60**, 618–626 (2016).
27. L. Del Longo, M. Ferrari, E. Zanghellini, M. Bettinelli, J. A. Capobianco, M. Montagna, and F. Rossi, "Optical spectroscopy of zinc borate glass activated by Pr^{3+} ions," J. Non-Cryst. Solids **231**(1-2), 178–188 (1998).
28. L. Lin, G. Chongfeng, J. Huan, L. Ting, and J. Jung-Hyun, "Green up-conversion luminescence in Yb^{3+}-Pr^{3+} co-doped $BaRE_2ZnO_5$ (RE = Y, Gd)," J. Rare Earths **31**(12), 1137–1140 (2013).
29. R. Balda, J. Fernández, A. Mendioroz, M. Voda, and M. Al-Saleh, "Infrared-to-visible upconversion processes in Pr^{3+}/Yb^{3+}-codoped KPb_2Cl_5," Phys. Rev. B **68**(16), 165101 (2003).
30. R. Woodward, D. Hudson, and S. Jackson, "Towards diode-pumped mid-infrared praseodymium-ytterbium-doped fluoride fiber lasers," in *Fiber Lasers XV: Technology and Systems*, (International Society for Optics and Photonics, 2018), 105120S.
31. Laércio, Gomes, D. Stuart, and Jackson, "Spectroscopic properties of ytterbium, praseodymium-codoped fluorozirconate glass for laser emission at 3.6μm," J. Opt. Soc. Am. B **30**(6), 1410 (2013).
32. M. F. H. Schuurmans and J. M. F. van Dijk, "On radiative and non-radiative decay times in the weak coupling limit," Physica A: Statistical Mechanics and its Applications **123**(1), 131–148 (1984).
33. B. R. Judd, "Optical Absorption Intensities of Rare-Earth Ions," Phys. Rev. **127**(3), 750–761 (1962).

Optics EXPRESS

34. L. V. G. Tarelho, L. Gomes, and I. M. Ranieri, "Determination of microscopic parameters for nonresonant energy-transfer processes in rare-earth-doped crystals," Phys. Rev. B **56**(22), 14344–14351 (1997).
35. D. E. McCumber, "Theory of Phonon-Terminated Optical Masers," Phys. Rev. **134**, A299–A306 (1964).
36. O. Henderson-Sapir, S. D. Jackson, and D. J. Ottaway, "Versatile and widely tunable mid-infrared erbium doped ZBLAN fiber laser," Opt. Lett. **41**(7), 1676–1679 (2016).
37. O. Henderson-Sapir, A. Malouf, N. Bawden, J. Munch, S. D. Jackson, and D. J. Ottaway, "Recent advances in 3.5 μm erbium-doped mid-infrared fiber lasers," IEEE J. Select. Topics Quantum Electron **23**(3), 6–14 (2017).